Molecular Crystals and Liquid Crystals
Publication details, including instructions for authors and subscription information:
http://www.tandfonline.com/loi/gmcl16

Search for Exciton Aggregates in Anthracene Crystals

V. A. Benderskii [a], V. Kh. Brikenstein [a], Ye. Ya. Misochko [a], N. A. Vidmont [b] & V. V. Korshunov [b]

[a] Institute of Chemical Physics, Academy of Sciences of the U.S.S.R., Chernogolovka, U.S.S.R.

[b] Institute of Solid State Physics, Academy of Sciences of the U.S.S.R., Chernogolovka, U.S.S.R.

Version of record first published: 14 Oct 2011.

To cite this article: V. A. Benderskii , V. Kh. Brikenstein , Ye. Ya. Misochko , N. A. Vidmont & V. V. Korshunov (1980): Search for Exciton Aggregates in Anthracene Crystals, Molecular Crystals and Liquid Crystals, 57:1, 47-64

To link to this article: http://dx.doi.org/10.1080/00268948008069818

Mol. Cryst. Liq. Cryst., 1980, Vol. 57, pp. 47–64
0026-8941/80/5701-0047$04.50/0

Search for Exciton Aggregates in Anthracene Crystals

V. A. BENDERSKII, V. KH. BRIKENSTEIN, and YE. YA. MISOCHKO

Institute of Chemical Physics, Academy of Sciences of the U.S.S.R., Chernogolovka, U.S.S.R.

and

N. A. VIDMONT and V. V. KORSHUNOV

Institute of Solid State Physics, Academy of Sciences of the U.S.S.R., Chernogolovka, U.S.S.R.

Various nonlinear phenomena observed in molecular crystals under intensive optical pumping (nonlinear fluorescence quenching, stimulated emission, pulsed heating and propagation of phonons) have been considered. Changes in anthracene crystals fluorescence spectra have been studied for pulse pumping intensities of 10^{20}–$5 \cdot 10^{22}$ cm^{-2} s^{-1}. Additional broadening of exciton bands occurs at intensities exceeding a certain initial level and has unusual kinetics: slow growth (broadening maximum is observed at a drop of the pumping pulse) and a considerably rapid drop (in the range of 1–3 ns). When the front of the crystal is illuminated with a probing pulse of low intensity emitted after finishing of the pumping pulse, a sharp threshold broadening of the bands is observed with the growth of the probing pulse, the probing pulse causing the broadening without practically heating the crystal. A reversible formation of defects under the action of intense UV pumping has been found. It is concluded that the observed "superheating-broadening" effects are caused by interaction of the Frenkel excitons.

FOREWORD

The study of the optical properties of crystals at high levels of optical pumping takes a special place among V. L. Broude's works. The investigations brought to light a number of nonlinear phenomena characteristic of organic molecular crystals, i.e. their stimulated emission, nonlinear fluorescence quenching, propagation and relaxation of nonequilibrium phonons under pulse pumping. Their main characteristics have been sufficiently well investigated by now in the works of both the Soviet and foreign scientists. This cannot be said about another expected phenomenon, the formation of aggregates of Frenkel excitons whose study is far from being completed.

We worked together with V. L. Broude on this difficult and interesting problem and know how much energy, inventiveness and inspiration he brought into this work.

Results of investigations and their discussion with V. L. Broude in the course of several years are a basis of this article dealing with the present state of the problem. We hope to attract attention by our work to this new field in the optics of molecular crystals.

INTRODUCTION

In a number of nonorganic crystals, when the critical density of Wanier excitons is reached ($\sim 10^{13}$–10^{14} cm^{-3}), their condensation occurs with the formation of electron-hole droplets (EHD).[1–3] For a gas of Frenkel excitons whose ionization energy is much greater than the interaction energy, the formation of dielectric exciton liquid droplets[4–6] may be expected under condensation, and not that of EHD. The theoretical possibility of the formation of biexcitons in molecular crystals was considered in Refs. 7 and 8. In view of the short-range (compared to the Coulomb one) interaction between small-radius excitons, the critical concentration necessary for condensation must be several orders higher than for Wanier excitons, i.e. 10^{16}–10^{18} cm^{-3}. Since the lifetimes of excitons in typical molecular crystals of anthracene and naphthalene is 10^{-9}–10^{-7} s, obtaining such high exciton densities requires high (up to 10^{27} cm^{-3} s^{-1}) densities of optical pumping acting for several nanoseconds and, naturally, it is accompanied by a number of side effects making difficult the detection of the phenomenon under discussion. Besides, as opposed to nonorganic crystals where at present a great number of direct experimental methods for the detection and study of EHD properties have been developed (light dissipation (Ref. 9), direct photo detection (Ref. 10), conductivity (Ref. 11), plasma resonance (Ref. 12), etc.) it is difficult to indicate methods of direct detection of exciton aggregates in molecular crystals. In particular, it is unlikely that the formation of dielectric exciton liquid droplets could result in a noticeable change of light dissipation, the appearance of conductivity or UV-absorption. In view of this, the researcher has actually only one source of information to judge the changes in the exciton subsystem, i.e. the change of the intensity and the shape of the exciton fluorescence bands depending on the level of pumping, temperature and time. However it is difficult to use these measurements to obtain immediately even indirect data on interaction of Frenkel excitons at their high density due to several accompanying effects caused by the high density of pumping.

The reaction of high concentrations of excitons in anthracene crystals at low temperatures is accompanied by the nonlinear fluorescence quenching (NFQ),[13-16] stimulated emission[17-20] and pulse heating.[21-23] The NFQ leads to a sublinear dependence of exciton concentration, n_s, on the light intensity ($n_s \propto I^{1/2}$), which additionally raises the required pumping levels and makes unavoidable the intensive generation of inequilibrium phonons due to emissionless conversion of light quanta in lower excitons zone. The change of the exciton band shape under these conditions may be caused by the changes of both the exciton and the phonon subsystem. Since the connection of the exciton band shape with the exciton-phonon interaction has not been studied quantitatively, an a priori separation of these two contributions appears impossible and special conditions of measurement are needed which guarantee low influence of the second effect.

The present work contains a brief analysis of all the obtained data on separation of the phonon and exciton contributions into the change of the shape and intensity of the anthracene crystals exciton fluorescence bands and a review of the influence of the reversible accumulation of photochemical defects over them.

1. ANTHRACENCE CRYSTALS FLUORESCENCE AT HIGH LEVELS OF OPTICAL PUMPING

1.1. Nonlinear fluorescence quenching

The reason for NFQ in molecular crystals is bimolecular recombination of excitons.[13,14] A quantitative description of NFQ is given in Refs. 14 and 15 where recombination rate constant γ is determined and it is shown that in anthracene crystals recombination is caused by a dipole-dipole interaction (the Förster radius R_0 is about 40 Å) which results in an energy transfer from one exciton to another with the formation of a higher vibration state with a doubled energy, the latter emissionlessly decaying into a lower exciton zone, and phonons, so that at each recombination act the energy of one exciton is transferred to a phonon subsystem, and at pumping levels of $I \gtrsim 10^{23}$ $\text{cm}^{-2}\,\text{s}^{-1}$ (for an absorption coefficient of $2 \cdot 10^4\ \text{cm}^{-1}$) when the quantum fluorescence yield is decreased by more than 10 times (compared to $I \to 0$), practically all the pumping energy is spent on the heating of crystals. In the range of 300–50 K, $\gamma \propto R_0^6$ and is independent of the exciton diffusion coefficient which grows as temperature decreases.[15] Below 40 K, γ decreases, at 10 K $\gamma = 5.10^{-9}\ \text{cm}^3\,\text{s}^{-1}$, which in Ref. 16 is explained by the transition to the flight regime of recombination of free excitons when their free path becomes greater than R_0. The exciton diffusion coefficient amounting to about 1 $\text{cm}^2\,\text{s}^{-1}$ in anthracene crystals at 10 K was found in Ref. 16 from the

NFQ curves measurements for different values of the pumping light absorption coefficient.

1.2 Stimulated emission

The stimulated emission of anthracene crystals occurs in the most intensive 23.692 cm^{-1} band of exciton fluorescence.[17] Its mechanism and connection with NFQ were investigated in Refs. 18–20. According to Ref. 18, the generation threshold by the pumping light intensity grows with an increase of the crystal thickness and a decrease of the illuminated surface, so that by changing these parameters, either NFQ or light generation may be observed in the selected I region. The data of Refs. 19 and 20 indicate that generation occurs at modes of a complete internal reflection of a plane-parallel anthracene plate along optically perfect channels with cross-sectional dimensions of $10^{-2} \times 10^{-4}\ \mathrm{cm}^2$. Generation light intensity in the channel reaches 200 MW cm^{-2} and produces a stimulated Raman scattering of the generation light at intramolecular vibration of 1403 cm^{-1}.[24,25] In Refs. 26 and 27, light generation in impurity anthracene crystals was studied when impurity pumping is effected by the exciton energy transfer. Simultaneous amplification of several electronic-vibrational impurity fluorescence bands is observed in anthracene crystals with a perylene impurity, which is caused by a restriction of transition due to the final ($\sim 10^{-10}$ s) lifetime of vibrational sublevels of the basic state. Development of generation in the 23.692 cm^{-1} band results in stabilization of exciton concentration, so that high n_s values may be reached only under conditions of its suppression. The latter is experimentally controlled by the absence of the amplification and change of the 23.692 cm^{-1} band shape differing from that of the other bands. Even in thin (1 μm) anthracene crystals stimulated emission is absent up to $I \lesssim 10^{23}\ \mathrm{cm}^{-2}\,\mathrm{s}^{-1}$ when the pumping spot dimensions do not exceed $0.3 \times 0.3\ \mathrm{mm}^2$.

1.3 Pulse heating of crystals

The temperature of the pumped region may be evaluated using the known temperature dependence of the enthalpy $\Delta H(T)$ of anthracene crystals.[28] Table I shows calculated temperature values of a thin ($kd < 1$) crystal without heat exchange for different values of exciton concentrations generated by a nitrogen laser pulse with a duration of $t_0 = 10$ ns. At low pumping levels in the absence of NFQ, the quantum yield of fluorescence ϕ is close to 1 and part of the energy w_1 is transferred into heat during decay of the higher vibrational state with an energy of $\hbar\omega$ (3.68 eV) into a lower zone (3.12 eV) and vibrational relaxation exciton in the basic state after optical transition. A decrease of ϕ with the growth of I conditioned by NFQ produces the additional heat

TABLE I

Adiabatic temperature of the anthracene crystal for various condensations of excitons[a]

n_s, cm^{-3}	ϕ	I, cm^{-2} s^{-1}	$T(w_1)$	$T(w_2)$	T
10^{16}	1.0	1.3×10^{20}	5.0	4.2	5.0
1.2×10^{17}	0.45	2.8×10^{21}	8.4	10.4	11.3
6.7×10^{17}	0.16	4.2×10^{22}	16	25	27
1.2×10^{18}	0.1	10^{23}	21	36	39

[a] The Thermostat temperature is 4.2 K.

source w_2. It follows from Table I that for $n_s \gtrsim 3 \cdot 10^{17}$ cm^{-3}, $w_2 > w_1$ and $T > 20$ K.†

For higher heat conductivity of the crystal and $kd \gg 1$, the required n_s values may be obtained at lower temperatures. In fact, according to Ref. 29, in anthracene crystals with a thickness $d = 2 \cdot 10^{-3}$ cm, for $I = 10^{23}$ cm^{-2} s^{-1}, $T = 24$ K instead of the calculated 39 K. A two-pulse method of measuring micron thick crystals heat conductivity was proposed in Ref. 21. In perfect anthracene crystals acoustic phonons propagate in a ballistic regime with a sonic speed $v \simeq 10^5$ cm · s^{-1}, their free path 1_{ph} exceeds 30 μm, so that the effective coefficient of heat conductivity exceeds 10^2 cm^2 s^{-1}. Heat exchange with the thermostat occurs during the times 10^{-4}–10^{-5} s. Later on the method of Ref. 21 was used in Refs 22 and 23 for studying the phonons' propagation regime. According to the theoretical model in Refs. 23 and 30, in the pumping absorption layer ($1/k \simeq 5 \cdot 10^{-5}$ cm), mainly Debye ($\omega \simeq \omega_d = k\theta_d/\hbar$, $\theta_d = 40$ cm^{-1})^{31} phonons are generated whose lifetime prior to decay (τ°_{ph}) does not exceed $1 \div 3 \cdot 10^{-10}$ s. During their decay, longer wave phonons ($\omega \simeq \omega_d/2$) with a greater lifetime are produced ($\tau_{\text{ph}} = \tau^\circ_{\text{ph}}(\omega_d/\omega)^5$) going from the $1/k$ layer into the crystal volume. Phonon propagation accompanied by further decay during which phonons of subsequent generations are produced with longer free paths, and a regime of quasiballistic or hydrodynamic transit from the front face to the back one appears, which is, in particular, detected by oscillations in the phonon density on these faces due to successive reflections. The subsequent processes of fusion of phonons and their interaction with equilibrium ones lead to the establishment of a new equilibrium temperature in the crystal. As the crystal thickness becomes smaller, the time for the establishment of a uniform spatial phonon distribution decreases.

---

† A decrease of heating without lowering n_s may be reached by the shortening of the pulse duration since under the NFQ conditions the lifetime of excitons decreases. For $t_0 = 2$ ns, the value $n_s = 10^{18}$ cm^{-3} corresponds to the heating up to 26 K.

1.4 Fluorescence spectra of anthracene crystals under high densities of excitons

It was found in Refs. 32 and 29 that at exciton concentrations exceeding the threshold value above $n_s^0 \simeq 10^{17}\,\mathrm{cm}^{-3}$ ($I_0 \gtrsim 5 \cdot 10^{21}\,\mathrm{cm}^{-2}\,\mathrm{s}^{-1}$), the width of all the anthracene exciton fluorescence bands starts to grow sharply as pumping increases. Broadening of the bands is accompanied by a decrease of the quantum yield of the fluorescence integrated over the spectrum. Special experiments were conducted for separation of the exciton and phonon contributions to the observed change of the band shape, the basic feature of the experiments being the changing of the exciton concentration with the level of the injected energy kept constant. In one series of the experiments an absorbing layer (heater) was applied to a part of the crystal surface and fluorescence spectra were compared at identical levels of the pumping absorbed in the crystal and in the heater. Proceeding from the findings of Refs. 29 and 32 it was concluded that threshold broadening of the exciton bands is caused by the changes in the exciton subsystem. In the light of the data on evolution of the phonon subsystem obtained later,[22,23] this conclusion requires additional evidence since the energetic and space distribution of the generated phonons under light absorption in the crystal and in the heater may be different if, for instance, the heater is injecting already Plank phonons into the crystal. A number of experiments conducted with this aim in view are discussed in the present work.

2 MEASUREMENT TECHNIQUE

2.1 Measurements of fluorescence spectra resolved in time

The experimental setup is shown in Figure 1. Optical pumping was performed with a nitrogen laser (3371 Å) with a repetition frequency of 100 Hz. The uniform excitation spot formed by a system of lenses and diaphragms had a diameter of 0.3 mm which guaranteed the absence of stimulated emission. A weakened pulse of the same laser was used for probing. It could be directed at both the front and the back faces of the crystal via a controlled optical delay line. The probing pulse spot size was somewhat smaller than that of the main pumping pulse; it was used for illuminating either the same part of the front face or the part of the back surface located just under the main pumping spot. Time scanning of the spectrum was performed with a 4-stage electron-optical converter on whose deviating plates serrated voltage was directed. The image was read out of the converter screen with a photomultiplier whose signal was registered with a recorder. The image of the same part of the screen was projected onto the photomultiplier cathode using the objective and the

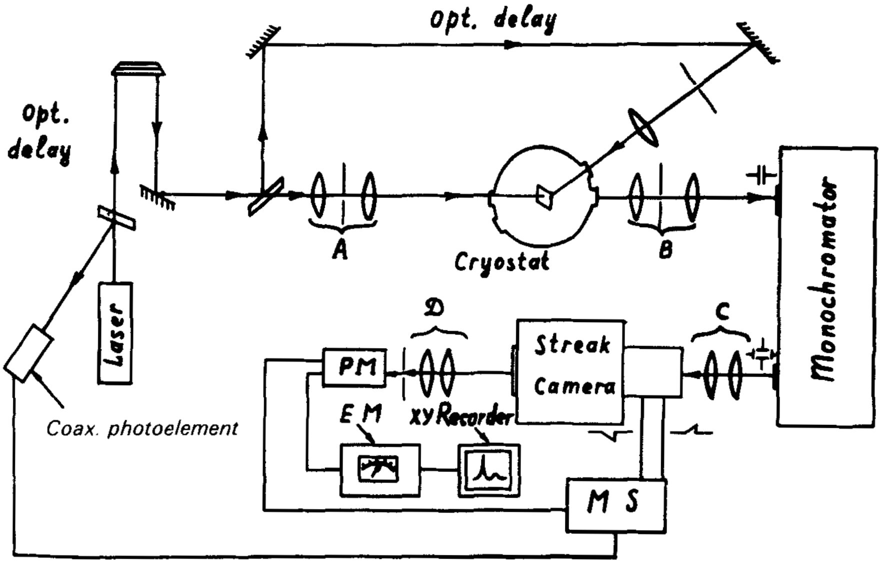

FIGURE 1 Block diagrams of the unit for investigating time-resolved fluorescence spectra. A = optical system for forming the exciton spot. B, C, D = optical system for the luminescence registration. MS = monitoring system. EM = electrometer. PM = photomultiplier.

diaphragm, the stroboscopic regime of recording being effected by directing the slowly changing voltage at the same pair of deviating plates at which the rapid serrated voltage was directed. The combination of the electronic-optical converter with a photomultiplier ensured high sensitivity of the test unit with the time resolution above 0.1 ns. Part of the measurements were carried out with the unit described in Ref. 24 where a high-speed photomultiplier with time resolution about 1 ns served as the emission receiver.

2.2 Measurements of temperature under pulse pumping

The crystal temperature under nanosecond pumping was determined by the broadening of the exciton fluorescence bands or by the change of the Debye–Waller factor, W, in the fluorescence spectrum of the tetracene impurity with a concentration of 10^{15}–10^{16} cm^{-3} which did not affect the shape of the exciton fluorescence bands. These "thermometers" were calibrated at low pumping levels and constant temperatures of the thermostat (Figure 2a) for each of the samples. The readings of both thermometers agreed with each other and the dependence $T(t, I)$ calculated from the pumping pulse shape and the temperature dependence of the crystal enthalpy when 1–2 μm thick crystals were heated with the absorbing layer (sprayed layer of copper phthalocyanine 0.1–0.2 μm thick in which the pumping light was weakened 30–50 times).

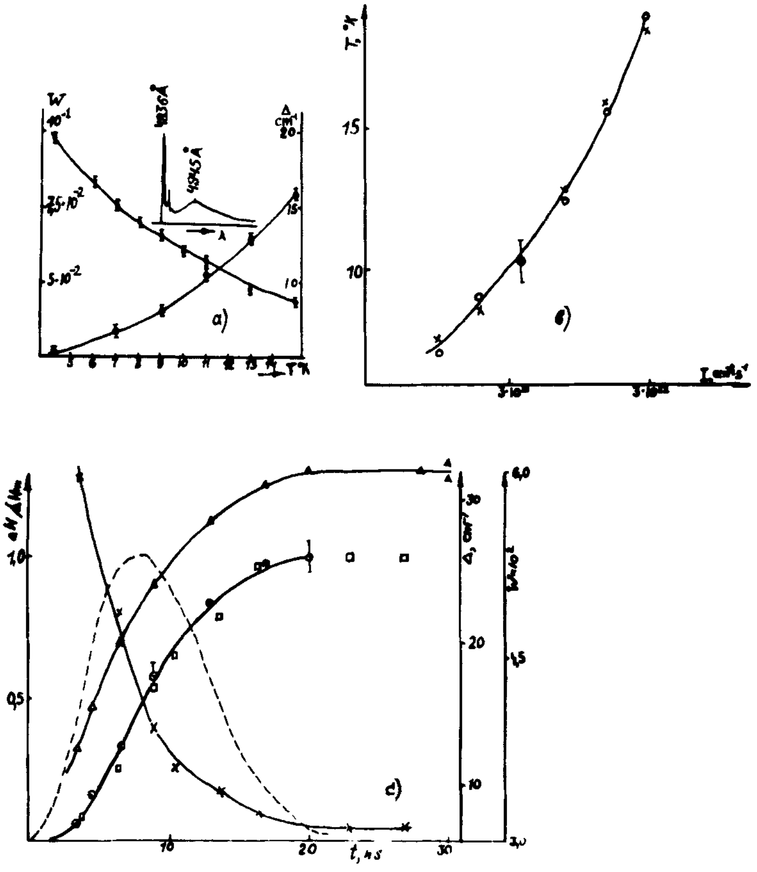

FIGURE 2 (a) Calibration of "internal thermometers," (○) = half-width of the 23.692 cm^{-1} band of anthracene (△), (●) = Debye–Waller factor of the tetracene impurity (W). In the upper part of the figure is shown the fluorescence spectrum of the tetracene impurity in an anthracene crystal at 5 K. (b) Dependence of the temperature of a thin ($d \simeq 1.5$ μm) anthracene crystal on the pumping intensity during excitation via a heater layer. (○) = readings of "anthracene" and (×) "tetracene thermometers." Measurements are in the maximum of the fluorescence pulse ($t_m = 8$ ns). Calculated dependence of crystal temperature is shown with the continuous curve. (c) Change of the half-width of the 23.692 cm^{-1} band (△) and the Debye–Waller factor of tetracene impurity (●) during heating of the crystal with thickness $d \simeq 1$ μm with a heater layer. The continuous curve (1) corresponds to the change in time of the absorbed pumping energy $\Delta H/\Delta H_m = \int_0^t f(t')dt'$, whose pulse shape $f(t)$ is shown with the dashed line. (○) and (□) correspond to values of $\Delta H/\Delta H_m$ recalculated from readings of the "anthracene" and "tetracene thermometers" respectively. Data of Figures 2b, c were obtained at thermostat temperature of 5 K.

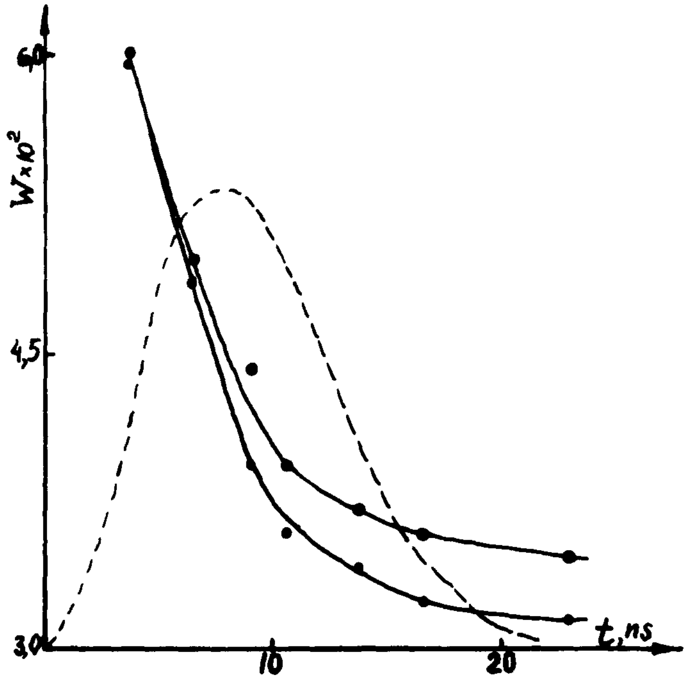

FIGURE 3 Change of the Debye–Waller factor of the tetracene impurity of 1 μm thick crystal under light absorption in the heater (●) and in the crystal (○). The thermostat temperature is 5 K.

Figure 2 shows the dependence on *I* of the measured and calculated (for the case of uniform heating) crystal temperature in the pumping pulse maximum. The change of the half-width of the exciton band 23.692 cm^{-1} and the Debye–Waller factor under heating with the absorbing layer in the process of pumping is shown in Figure 2c. The same figure demonstrates the close correspondence of the crystal enthalpy change calculated by the readings of both thermometers with the change in time of the energy absorbed by the heater layer. From the data of Figure 2 it follows that in crystals 1–2 μm thick the uniform space distribution of phonons injected by the heater results in the establishment of temperature in the course of times shorter than 1 ns.

The accuracy of the tetracene thermometer readings makes possible the next step, i.e. determination of the temperature establishment dynamics under pumping of the exciton subsystem. Figure 3 demonstrates the change of the Debye–Waller factor during absorption of light in the crystal and the heater. Coincidence of these curves with an accuracy of 2–3 ns† indicates that

---

† The difference of the $W(t)$ curves in the 2–3 ns range may result from the change of the energy fraction transferred to phonons due to the change in time of the NFQ factor.

in crystals of the above thickness the temperature is established in times shorter than 2–3 ns and under excitation of the exciton subsystem. Note also that at $t \geqslant 16$ ns, in accordance with the laser pulse shape, crystal temperature is actually constant.

3 RESULTS AND DISCUSSION

Broadening of the exciton bands in time under various pumping conditions shown in Figure 4 is a non-monotonous one. Maximum of broadening is observed at the drop of the pumping pulse. Narrowing of bands to corresponding crystal temperatures occurs in the range of 2–3 ns at times when, according to data of Figure 3, crystal temperature is constant. Additional broadening, as in Refs. 28 and 32, appears under pumpings exceeding a definite initial level and has unusual kinetics: slow growth and a considerably more rapid drop. When the thermostat temperature grows, additional broadening occurs in the range of high pumpings. It is not observed for $I \lesssim 3 \cdot 10^{22}$ cm^{-2} s^{-1} at the thermostat temperatures over 20 K.

If, after the pumping pulse ($t \geqslant 20$ ns), when the width of the exciton bands decreases to a constant value, a low intensity probing pulse is directed at the crystal,† the shape of the exciton bands is considerably different during the illumination of the front and back faces. When the front face is illuminated, a sharp threshold broadening of bands occurs which is absent during the illumination of the back face (Figure 5) when broadening corresponds to temperature increase. Threshold values I_p of the probing pulse corresponding to the beginning of the broadening are several times lower than that for the main pulse, so that the probing pulse produces sharp broadening of the exciton bands without practically heating the crystal.

Thus, nonequilibrium phonons have nothing to do with the observed additional broadening of the exciton bands. However, the presence of this broadening at exciton concentrations 4–5 times lower than in the pumping pulse maximum‡ makes one assume that broadening of exciton bands may be associated not with exciton density changes, but with accumulation of reversible§ photochemical defects appearing under powerful UV-pumping

---

† Crystals 2–3 μm thick were chosen for these measurements since in such samples uniform space distribution of phonons is established during the pumping pulse time, whereas excitons, due to their short diffusion length ($\lesssim 1$ μm at 10 K[16]) do not reach the back face.

‡ The slow drop of exciton concentration at the pumping pulse tail is associated with the presence of NFQ leading to the dependence $n_s \propto I^{1/2}$ close to the maximum $f(t)$ and $n_s \propto I$ in the range of pumping drop. At $t = 20$ ns, $f(t) \simeq 0.05$, $f(t_m) = 1$.

§ It is indicated in Ref. 29 that at stroboscopic registration with the averaging signal by $\sim 10^3$ pumping pulses, any accumulation of spectrum distortions irreversible during over 10^{-2} s (time between the pulses) must lead to irreproducibility of results with prolonged measurements, which has not been detected.

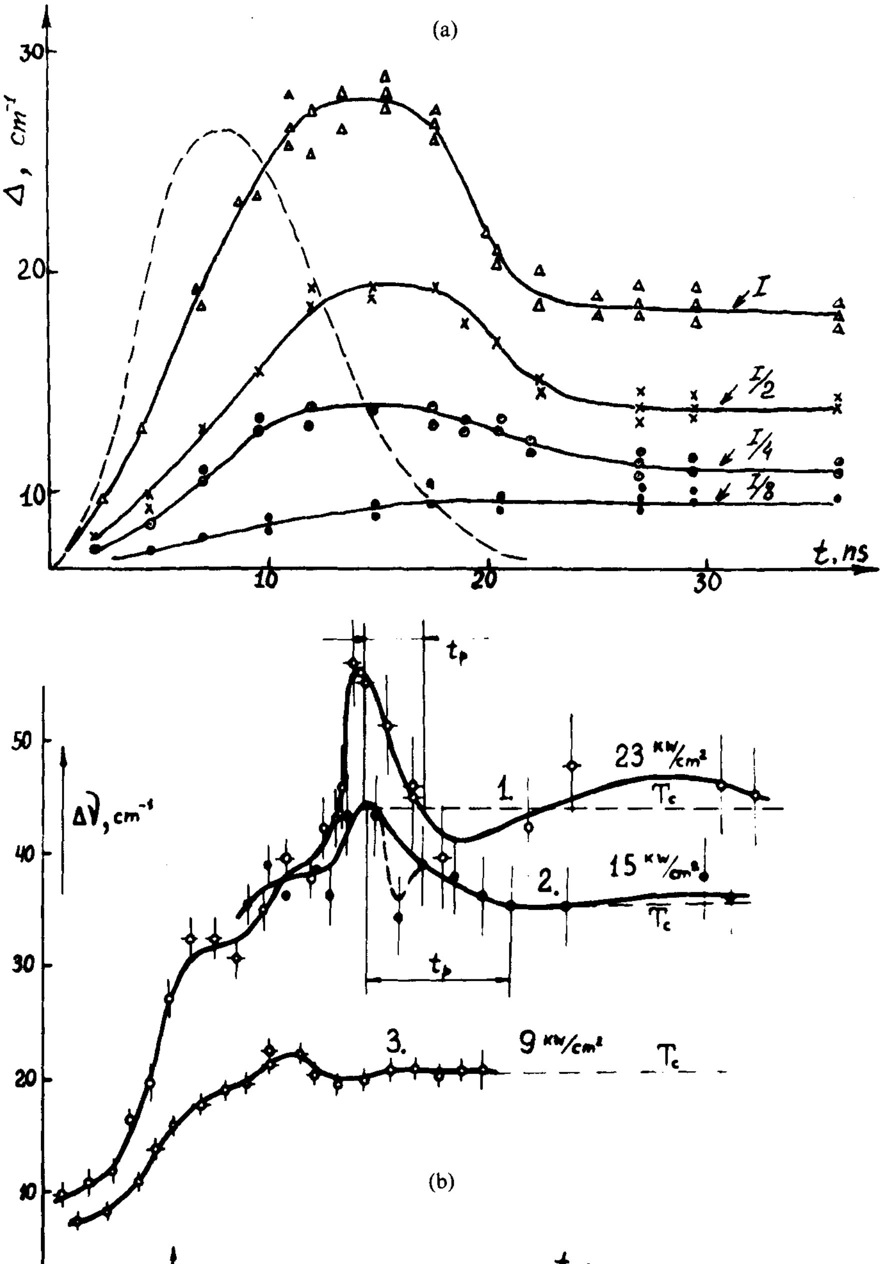

FIGURE 4 Change in time of the half-width of the 23.692 cm^{-1} band at various pumping levels. (a) Measurements with photomultiplier. The crystal thickness is 1.5 μm, maximum pumping $I = 3 \cdot 10^{22}$ cm^{-2} s^{-1}. (b) Measurements with electron-optical converter. $d \simeq 0.8$ μm. 1 – I = 25 kW/cm^2, 2 – 15 kW/cm^2, 3 – 9 kW/cm^2. The thermostat temperature is 5 K.

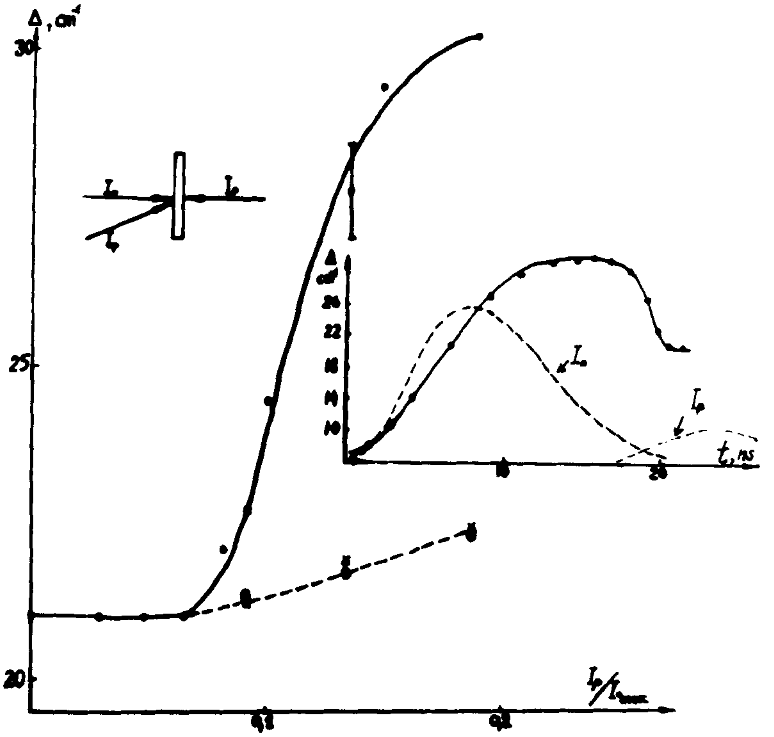

FIGURE 5 Dependence of the half-width of the 23.692 cm^{-1} band on the intensity of the probing pulse I_p. (●) = for illumination of the front face, (○) for illumination of the back face. The thermostat temperature is 5 K. (×) = dependence of Δ on I_p with the main pulse switched off, the thermostat temperature is 18.5 K. In the insert to the figure, the relative position of the main and probing pulses (dashed curves) is shown, the arrow indicates the time moment when the $\Delta(I_p)$ dependence was measured.

and distorting the exciton fluorescence spectrum. In order to detect the reversible formation of photochemical defects the two-pulse technique was employed.[33,34] Figure 6 shows the dependence of the relative change of the fluorescence pulse amplitude (η) excited by the probing pulse on the intensity of the main pumping for the delay time $t_d = 50$ ns (Figure 6a) and the dependence $\eta(t_d)$ at 300 K. The growth of η with I indicates the decrease of the quantum yield of fluorescence after powerful UV-irradiation of anthracene crystals which exists for about 10^{-6} s and is due to the formation of exciton capture centers with a lifetime of about 10^{-6} s. The decrease of the fluorescence quantum yield due to crystal heating and temperature quenching at 300 K is unimportant.[14] Similar measurements at the thermostat temperature of 4.2 K were made in Ref. 34. In Figure 7 are given dependences of $\eta(I)$ at various temperatures showing that with temperature decreasing the change

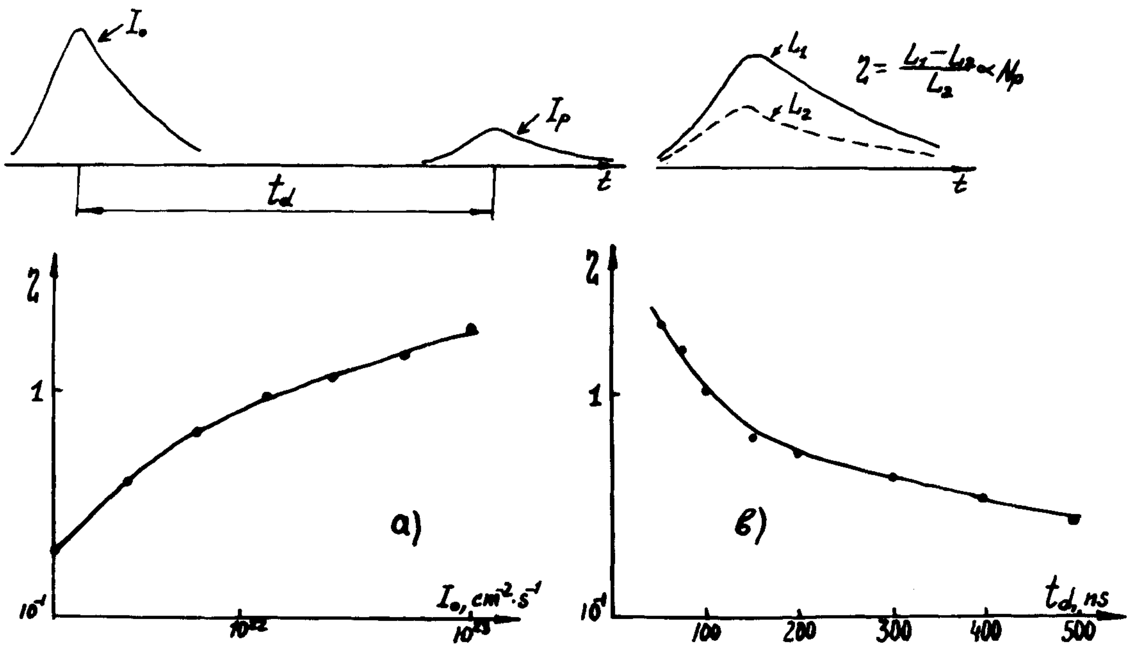

FIGURE 6 (a) dependence of relative decrease of the quantum yield of the defects (η) on intensity of the main pulse (t_d = 50 ns), (b) dependence $\eta(t_d)$. In the upper part of the figure is shown a sketch of the two-pulse method of detecting photochemical defects (L_1 and L_2 = amplitude values of fluorescence pulses induced by the probing pulse, with the main pulse switched off and on, respectively. The fluorescence integrated over the spectrum is measured.

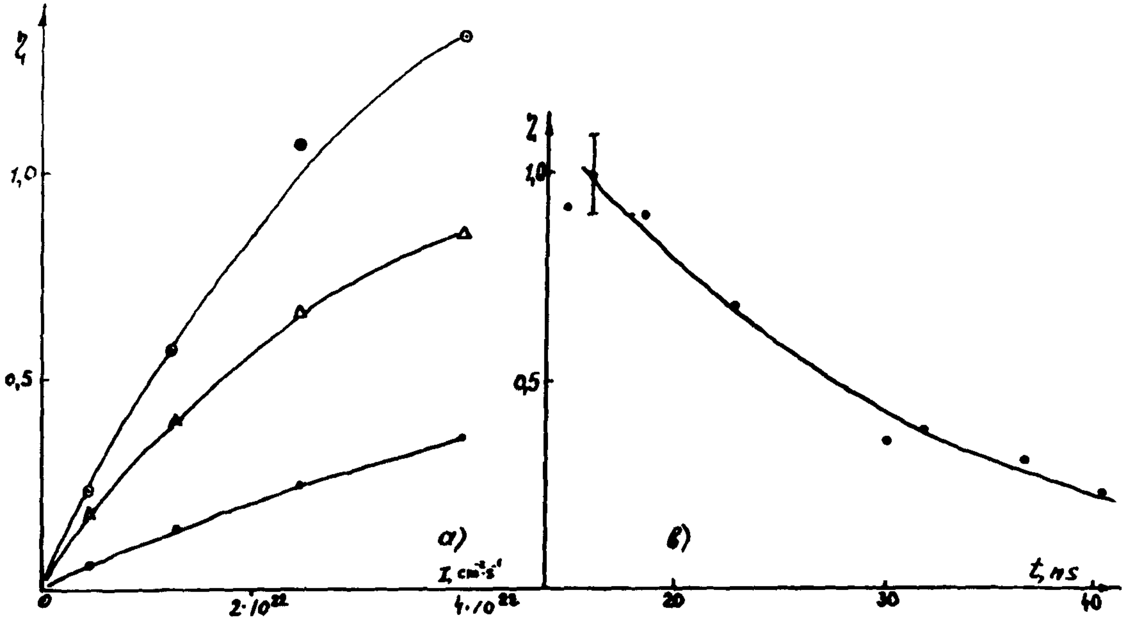

FIGURE 7 (a) The dependence $\eta(I)$ for various thermostat temperatures. (○) = 300 K, (△) = 77 K, (●) = 5 K. Measurements for t_d = 30 ns. (b) The dependence $\eta(t)$ for $I \simeq 4 \cdot 10^{22}\ \mathrm{cm}^{-2}\ \mathrm{s}^{-3}$. The thermostat temperature is 5 K.

of the quantum yield of exciton fluorescence diminishes and exists for shorter times. At 4.2 K the effect practically disappears for $t_d \gtrsim 100$ ns and the initial part of the η drop agrees with the characteristic time of about 20 ns (Figure 7b).† With typical values of the rate constant of exciton capture by the impurity ($\sim 10^{-8}\,\mathrm{cm}^3\,\mathrm{s}^{-1}$), concentration of the formed photochemical defects explaining the observed change of the fluorescence quantum yield has the order $10^{16}\,\mathrm{cm}^{-3}$ under pumping of $3 \cdot 10^{22}\,\mathrm{cm}^{-2}\,\mathrm{s}^{-1}$.‡

Formation of these defects may undoubtedly result in the distortions of the exciton shapes growing as their concentration increases. The latter, judging by the lifetimes of these defects, should monotonously increase in the course of the main pumping pulse and reach a maximum by its end which correlates with the observed growth of the band width. However, this cannot explain the sharp drop of additional broadening in the range of $t \simeq 18$–20 ns where defect concentration is maximum, since the drop of $\Delta(t)$ must occur cymbately with the change of $\eta(t)$, whereas, according to data of Figures 4, 5, 7, characteristic times of these dependences differ by an order. According to Figure 7b, in the range of 16–20 ns where additional broadening disappears, the change of $\eta(t)$ does not exceed 1.2 times. Unexplainable in this assumption remains also the threshold increase of the width with the growth of I_p which in itself practically does not form quenching centers ($\eta < 0.1$).

Thus results of the present work support the conclusion in Refs. 29 and 32 about the connection of additional broadening with interaction of Frenkel excitons at their high concentration. If, similar to Ref. 29, we assume that the observed fluorescence spectrum corresponds to overlapping of narrower exciton bands and wide bands of the new luminescence, we can separate a band of new luminescence in the range of the sharp drop of $\Delta(t)$. It is also assumed that the exciton band shape corresponds to the fluorescence spectrum measured in the range of $t > 22$ ns where the half-width of vibration bands remains constant (Figure 4). This assumption should not considerably affect the band separation results since, as mentioned above, at times $t \gtrsim 17$ ns crystal temperature practically does not change. The results of separation performed with a computer by the method of two-stage approximation are shown in Figure 8a. When processing the experimental curves, the error related to the noises was taken into account (the signal/noise ratio was approximately 20:1). In Figure 8b is shown the dependence of integral intensity of the new luminescence (S_k) on the integral intensity of exciton

---

† The change in the $t \lesssim 20$ ns range was found in Ref. 34 from an analysis of the fluorescence pulse shape with independently measured values of the lifetimes of excitons and the NFQ in the same sample.

‡ For different crystals the η value varied in the range of the factor of 2.

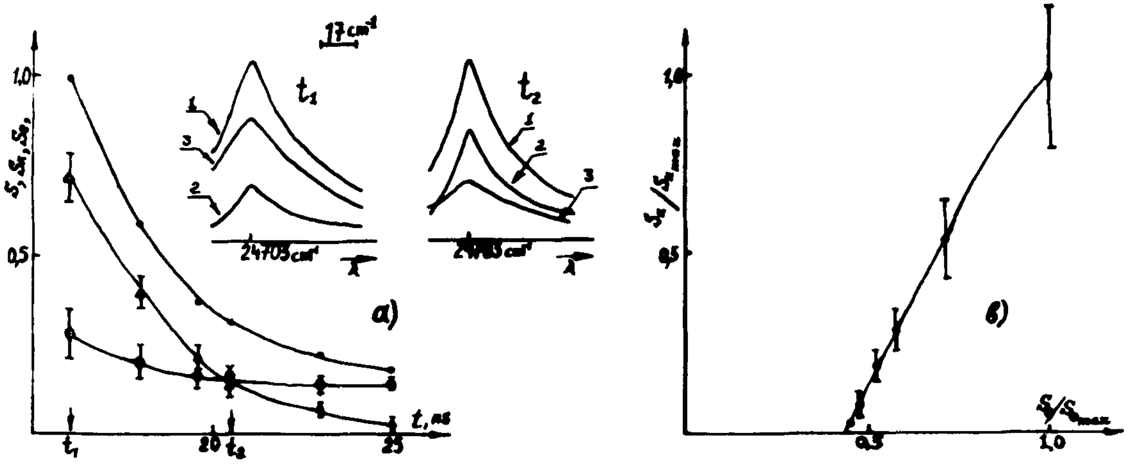

FIGURE 8 (a) Separation of bands performed by the method of double-stage approximation is shown in the upper part of the figure. 1 = enveloping, 2 = exciton, and 3 = new luminescence bands. In the lower part of the figure is shown the change in time of the integral from the band 24.703 cm^{-1} (S) – (●), of the integral from new luminescence band (S_k) – (△) and of the integral from the exciton band (S_e) – (○), ($S_k + S_e = S$). Integrating was performed in the range of $\Delta\nu = 80$ cm^{-1}. It was assumed during separation that the band measured at $t = 25$ ns corresponds to the exciton luminescence.

luminescence (S_e). This dependence is seen to be a sharply threshold one, as in the case of measurements with a probing pulse (Figure 5).

The threshold character of the observed dependences (Figures 5, 8) makes it possible to assume that the exciton interaction is a collective one. However, proceeding from the data available to date, it is impossible to reach an unambiguous conclusion concerning the character of this interaction. In particular, we cannot separate two possibilities: either, as was assumed in Ref. 29, fine drops of exciton liquid having a radius of 10^{-6} cm and an excitational concentration of the order of $10^{19}\,\mathrm{cm}^{-3}$ are formed, or exciton-impurity complexes appeared. In the first case it is difficult to explain the kinetics of the new luminescence, and in the second one, the threshold character of the observed dependences. Insufficiently clear remains the role of the photochemical defects which cannot by themselves explain the observed features of the new luminescence, but nevertheless may play a certain part in the observed effects, and, in particular, serve as centers close to which the formation of exciton aggregates occurs. Finally, the present study does not take into account a number of undoubtedly important details, such as anisotropy of the motion of excitons. In principle, the exciton condensation process should be a sharply anisotropic one, as at helium temperatures the motion of excitons in anthracene crystals is close to a unidimensional one (along the **a** axis) due to the non-analyticity of the zone and possess a large effective mass along the **c** axis.[35] The circumstances of interaction of Frenkel excitons and formation of exciton aggregates require further experimental and theoretical investigations.

Acknowledgments

The authors are grateful to I. B. Levinson, A. A. Ovchinnikov, and Ye. F. Sheka for useful discussion of the work.

References

1. L. V. Keldysh, Eksitony v poluprovodnikakh, *Izd. Nauka* (Moskva 1971).
2. V. S. Bagayev, N. V. Zamkovets, L. V. Keldysh, N. N. Sibeldin and V. A. Tsetkov, *Zh. eksper. teor. Fiz.*, **70**, 150 (1976).
   Ya. E. Pokrovskii, *Phys. Stat. Solidi* (*a*), **11**, 385 (1972).
3. V. G. Lysenko, V. I. Revenko, T. G. Tratas, and V. B. Timofeyev, *Zh. eksper. teor. Fiz.*, **68**, 335 (1975).
4. D. Fox, Eighth Molecular Crystal Symposium, Santa Barbara, California, USA.
5. S. D. Stojanovic, I. P. Setrajacic, and B. S. Tosic, *Phys. Stat. Sol.* (*b*), **79**, 443 (1977).
6. V. M. Agranovich and M. D. Galanin, Perenos energii electronnogo vozbuzhdeniya v kondensirovannykh sredakh, *Izd. Nauka* (Moskva 1978), Chaps. 4, 6.
7. N. A. Yefremov, *Fiz. tverd. Tela*, **17**, 1895 (1975).
8. C. Mavroyanis, *Phys. Rev. B*, **16**, 2871 (1977).
9. Ya. Ye. Pokrovskii and K. I. Svistunova, *Pis'ma Zh. Exper. Teor. Fiz.*, **13**, 297 (1971).

10. I. P. Wolfe, W. L. Hansen, E. E. Haller, R. S. Markiewicz, C. Kittel, and C. D. J. Jeffries, *Phys. Rev. Lett.*, **34**, 1292 (1975).
11. V. M. Asnin, A. A. Rogachev, and N. I. Sablina, *Pis'ma Zh. Exper. Teor. Fiz.*, **11**, 162 (1970).
12. V. S. Vavilov, V. A. Zayats, and V. N. Murzin, *Pis'ma Zh. Exper. Teor. Fiz.*, **10**, 314 (1969).
13. N. A. Tolstoi and A. P. Abramov, *Fiz. tverd. Tela*, **9**, 340 (1967).
14. S. D. Babenko, V. A. Benderskii, V. I. Goldanskii, A. G. Lavrushko, and V. P. Tychinskii, *Phys. Stat. Solidi* (*b*), **45**, 97 (1971).
15. V. A. Benderskii, V. Kh. Brikenstein, A. G. Lavrushko, and P. G. Filippov, *Phys. Stat. Solidi* (*b*), **86**, 449 (1978).
16. V. A. Benderskii, V. Kh. Brikenstein, A. I. Burstein, A. G. Lavrushko, and P. G. Filippov, *Phys. Stat. Sol.* (b), (1979, in print).
17. M. D. Galanin, Sh. D. Khan-Magometova, and Z. A. Chizhikova, *Pis'ma Zh. Exper. Teor. Fiz.*, **16**, 141 (1972).
18. V. A. Benderskii, V. Kh. Brikenstein, V. L. Broude, and A. G. Lavrushko, *Pis'ma Zh. Exper. Teor. Fiz.*, **17**, 472 (1973).
19. H. S. Avanesyan, V. A. Benderskii, V. Kh. Brikenstein, V. L. Broude, L. A. Korshunov, A. G. Lavrushko, and I. I. Tartakovskii, *Mol. Cryst. and Liq. Cryst.*, **29**, 165 (1974).
20. V. A. Benderskii, V. Kh. Brikenstein, V. L. Broude, L. A. Korshunov, A. G. Lavrushko, and I. I. Tartakovskii, *Optika i Spektroskopiya*, **39**, No. 1 (1975).
21. V. A. Benderskii, V. Kh. Brikenstein, V. L. Broude, and A. G. Lavrushko, *Solid State Commun.*, **15**, 1235 (1974).
22. V. L. Broude, N. A. Vidmont, V. V. Korshunov, I. B. Levinson, A. A. Maksimov, and I. I. Tartakovskii, *Pis'ma Zh. Exper. Teor. Fiz.*, **25**, 285 (1977).
23. V. L. Broude, N. A. Vidmont, D. V. Kazakovtsev, V. V. Korshunov, I. B. Levinson, A. A. Maksimov, I. I. Tartakovskii, and V. P. Yashnikov, *Zh. Exper. Teor. Fiz.*, **74**, 314 (1978).
24. O. S. Øvanesyan, V. A. Benderskii, V. Kh. Brikenstein, V. L. Broude, A. G. Lavrushko, I. I. Tartakovskii, and P. G. Filippov, *Kvantovaya elektronika*, **4**, 725 (1977).
25. H. S. Avanesyan, V. A. Benderskii, V. Kh. Brikenstein, and A. G. Lavrushko, *Phys. Stat. Solidi* (*a*), **27**, K77 (1975).
26. H. S. Avanesyan, V. A. Benderskii, V. Kh. Brikenstein, V. L. Broude, and A. G. Lavrushko, *Phys. Stat. Solidi* (*a*), **19**, K121 (1973).
27. H. S. Avanesyan, V. A. Benderskii, V. Kh. Brikenstein, A. G. Lavrushko, and P. G. Filippov, *Phys. Stat. Solidi* (*a*), **30**, 781 (1975).
28. P. G. Goursot, H. L. Gierdnar, and E. F. Westrum, *J. Phys. Chem.*, **74**, 2538 (1970).
29. V. A. Benderskii, V. M. Beskrovnyi, V. Kh. Brikenstein, V. L. Broude, A. G. Lavrushko, and A. A. Ovchinnikov, *Zh. Exper. Teor. Fiz.*, **72**, 106 (1977).
30. D. V. Kazakovtsev, and I. B. Levinson, *Pis'ma Zh. Exper. Teor. Fiz.*, **27**, 194 (1978).
31. U. Lutz, Gitterdynamik von Antrazen, Dissertationarbeit (Zürich, 1970).
32. V. A. Benderskii, V. Kh. Brikenstein, V. L. Broude, and I. I. Tartakovskii, *Pis'ma Zh. Exper. Teor. Fiz.*, **22**, 332 (1975).
33. V. A. Benderskii, V. Kh. Brikenstein, and A. G. Lavrushko, All-Union Conference on Photochemistry, 1977, (Synopses of reports, in Russian).
34. V. L. Broude, N. A. Vidmont, and V. V. Korshunov, *Phys. Stat. Solidi* (*b*), **90**, K53 (1978).
35. V. M. Agranovich, Teoriya eksitonov, *Izd. Nauka* (Moskva, 1968) Chap. 2.